SPARC-FEL-03/001
6 Jun 2003

SPARC FEL WORKING POINT AND UNDULATOR CONFIGURATION

F.Ciocci, G. Dattoli, A. Doria, G.P. Gallerano, L. Giannessi, E. Giovenale,
G. Messina, L. Mezi, P.L. Ottaviani[1], L. Picardi, M. Quattromini, A. Renieri, C. Ronsivalle

ENEA – C. R. Frascati – V. E. Fermi 45 – 00044 Frascati – Italy
*(1) ENEA – C. R. Ezio Clementel- Via Martiri di Monte Sole 4 – **40129** Bologna - Italy*

Abstract

In this note we discuss the SPARC FEL working point and present an analysis of possible undulator configurations.
The analysis we develop is relevant to the problems associated with the saturation length, we do not mention those due to the e-beam transport to the undulatorwich will be discussed in a dedicated report.

SPARC FEL WORKING POINT AND UNDULATOR CONFIGURATION

F. Ciocci, G. Dattoli, A. Doria, G. P. Gallerano,
L. Giannessi, E. Giovenale, G. Messina, L. Mezi,
P. L. Ottaviani, L. Picardi, M. Quattromini, A. Renieri
and C. Ronsivalle

ENEA Frascati June 6, 2003

0.1 INTRODUCTION

In this note we discuss the SPARC FEL working point and present an analysis of possible undulator configurations.

The analysis we develop is relevant to the problems associated with the saturation length, we do not mention those due to the e-beam transport to the undulator, which will be discussed in a dedicated report.

We will orient the first part of the discussion using an analytical formula for the saturation length, which includes the effect of the beam qualities and of the diffraction.

The formula is given below[1]

$$\begin{aligned} L_s &= \frac{\lambda_u}{4\pi\sqrt{3}\rho_D\chi}\left[\ln(9\frac{P_F}{P_0})+1\right] \\ P_F &= 1.67\eta(\chi)\rho_D P_E \end{aligned} \tag{1}$$

where λ_u is the undulator period, ρ_D is the Pierce parameter, including diffraction contributions, χ is a function accounting for the inhomogeneous broadening effects due to emittances and to the energy spread and P_E is the e-beam power, P_0 is the input seed power and $\eta(\chi)$ is the inhomogeneous broadening contribution to the global efficiency.

By denoting with ρ the 1-d Pierce parameter, we have

$$\begin{aligned} \rho_D &= \left[(1+\widetilde{\mu}_x^D)(1+\widetilde{\mu}_y^D)\right]^{-\frac{1}{6}}\rho \\ \chi(\widetilde{\mu}_\varepsilon,\widetilde{\mu}_x,\widetilde{\mu}_{x'},\widetilde{\mu}_y,\widetilde{\mu}_{y'}) &= \frac{\chi(0,\widetilde{\mu}_x,\widetilde{\mu}_{x'},\widetilde{\mu}_y,\widetilde{\mu}_{y'})\exp(-c\widetilde{\mu}_\varepsilon^2)}{1+0.185\frac{\sqrt{3}}{2}\chi(0,\widetilde{\mu}_x,\widetilde{\mu}_{x'},\widetilde{\mu}_y,\widetilde{\mu}_{y'})\widetilde{\mu}_\varepsilon^2} \\ \chi(0,\widetilde{\mu}_x,\widetilde{\mu}_{x'},\widetilde{\mu}_y,\widetilde{\mu}_{y'}) &= \frac{1+a(\widetilde{\mu}_x^2+\widetilde{\mu}_{x'}^2+\widetilde{\mu}_y^2+\widetilde{\mu}_{y'}^2)+b(\widetilde{\mu}_x+\widetilde{\mu}_{x'}+\widetilde{\mu}_y+\widetilde{\mu}_{y'})}{\sqrt{(1+\widetilde{\mu}_x^2)(1+\widetilde{\mu}_{x'}^2)(1+\widetilde{\mu}_y^2)(1+\widetilde{\mu}_{y'}^2)}} \end{aligned} \tag{2}$$

with a,b,c constants given by $(a=0.318/2, b=-0.132/2, c=3.4\cdot10^{-2})$, the coefficients $\widetilde{\mu}$ are the inhomogeneous broadening parameters, which in terms of the emitances $(\varepsilon_{x,y})$, relative energy spread (σ_ε), of the Twiss parameters $(\beta_{x,y},\gamma_{x,y})$, of the undulator strength K and of the beam energy γ, write

$$\begin{aligned} \widetilde{\mu}_{\eta'} &= \frac{1}{\rho_D}\frac{\gamma^2\varepsilon_\eta}{(1+\frac{K^2}{2})\lambda_u\beta_\eta}, \mu_\eta = \frac{1}{\rho_D}\frac{\gamma^2\Omega_\eta^2\varepsilon_\eta}{(1+\frac{K^2}{2})\gamma_\eta}, \widetilde{\mu}_\varepsilon = \frac{2\sigma_\varepsilon}{\rho_D}, \\ \Omega_\eta &= \frac{\pi K}{\gamma\lambda_u} \end{aligned} \tag{3}$$

Table 1: SPARC e-beam parameters, according to [2].

E	155.3MeV
I	85A
σ_ε	$0.6 \cdot 10^{-3}$
$\varepsilon_{x,y}$(normalized)	1mm·mrad

The inclusion of the diffractive effects through the parameter ρ_D are obtained by noting that the longitudinal mode transverse size in SASE FEL device is just given by

$$\begin{aligned} \Sigma_\eta &= \beta_\eta \varepsilon_\eta \sqrt{1+\widetilde{\mu}_\eta^D}, \\ \widetilde{\mu}_\eta^D &= \frac{\lambda_r \lambda_u}{(4\pi)^2 \beta_\eta \rho \varepsilon_\eta}, \lambda_r = \frac{\lambda_u}{2\gamma^2}(1+\frac{K^2}{2}) \end{aligned} \tag{4}$$

with $\widetilde{\mu}_\eta^D$ accounting for the diffraction contributions, which reflect into the SASE dynamics with an effective reduction of the ρ parameter, according to the prescription given in eq.(2).

The function $\eta(\chi)$, yielding the dependence of the output power on the beam qualities, has been derived from the analysis of the numerical data and the best fit yields

$$\eta(\chi) \simeq e^{-\frac{1-\chi}{\chi^2}} + \sqrt{2}(1-\chi)\chi^2 \tag{5}$$

According to the above formula and to the parameters of Tabs. 1,2, (see [2]) we get the results shown in Fig. 1, which report the saturation length vs β, includes the comparison with the Ming Xie formula and the case in which the diffraction contributions are neglected.

It is evident that diffraction plays a major role in determining the saturation length, furthermore, if we choose an undulator with the parameters reported in Tab. 2, focusing in both planes, we obtain, for an average $\beta = 1.55$m, $\rho = 5.2667 \cdot 10^{-3}$ and 0.5W as input power, a value of L_s around 10.53m.

The above formula has two major drawbacks:

1. it assumes the undulator focusing in both planes and constant β values inside the undulator;

2. it assumes the undulator as a continuum, without drift sections necessary for the inclusion of focusing quadrupoles, to compensate free propagation and small defocusing inside the undulator.

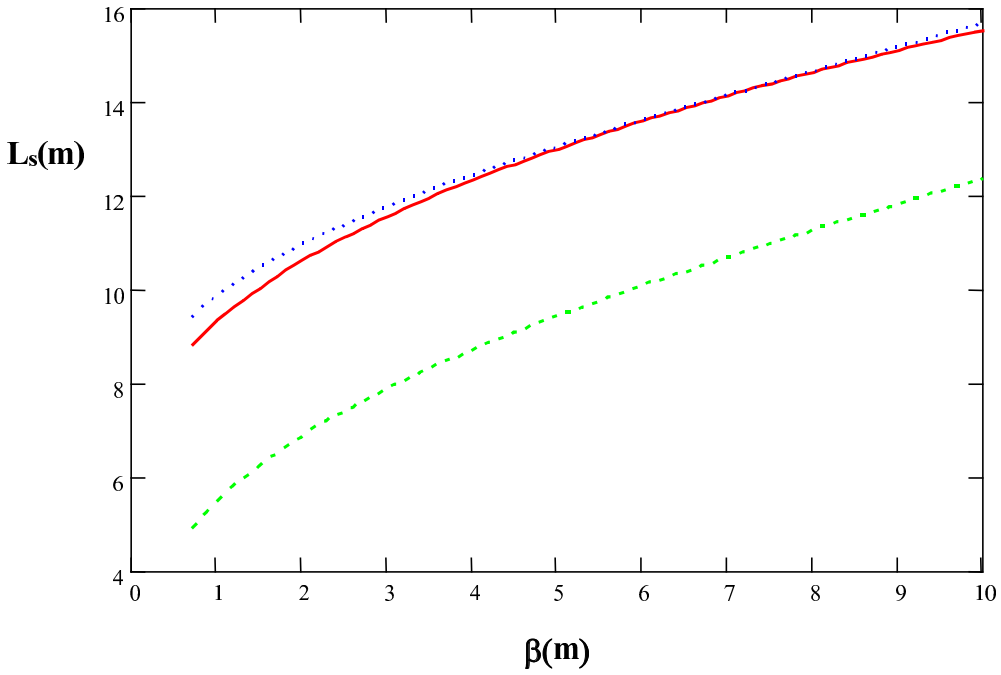

Figure 1: Saturation length vs β for the parameters in Tabs. 1,2. Solid line Ming Xie formula, dotted line eq. (1), dashed line eq. (1) without the diffraction effects.

Table 2: SPARC undulator parameters, according to [2].

λ_u	3cm
K	2
M	4
h	1.5cm

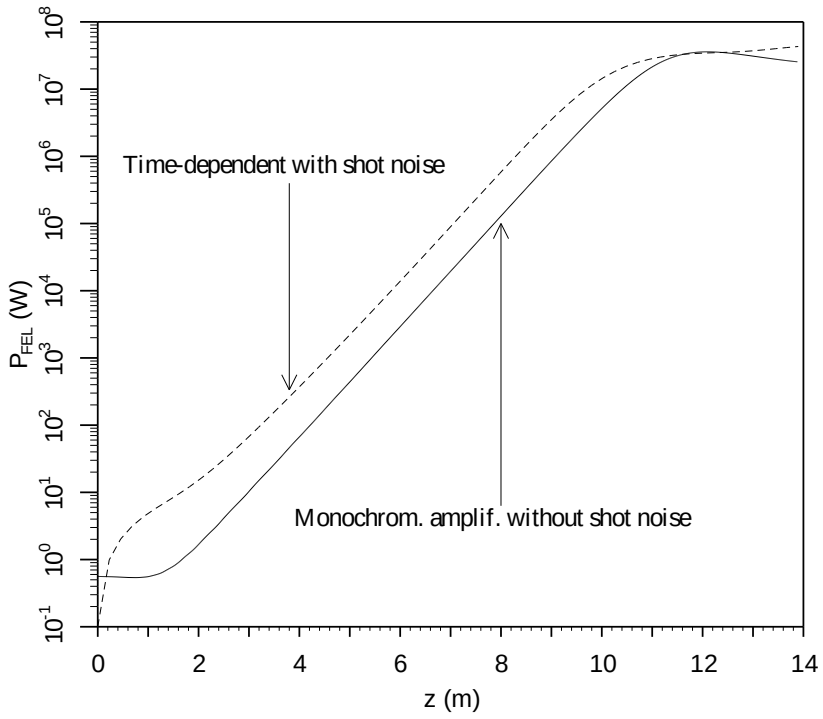

Figure 2: FEL power evolution vs the saturation distance. Ginger simulation input parameters from Tabs. 1,2, undulator focusing in both transverse directions, no drift sections for additional focusing.

In addition it does not include the initial e.m. mode size blow up due to diffraction and the free diffraction in the drift sections, which imply an uncompensated growth of the optical field and thus a loss of the bunching efficiency after each section.

The effect of the β oscillations and of the initial mode size growth can be accounted for by evaluating the saturation length for a β two times larger than the actual average value, if the value we have previously quoted is just an average value, we get from eq. (1) for $\beta \simeq 3.1$m a corresponding saturation length of 11.85m.

This ansatz is confirmed by the results of Fig. 2, where we have reported a Ginger simulation, for a FEL SASE operating with the parameters of Tabs. 1,2 and with a non-segmented undulator focusing in both transverse directions.

The saturation length is in close agreement with the prediction obtained choosing the previously quoted value of β and the value of ρ, extracted from

Table 3: VISA parameters.

E	83.8MeV
I	200A
σ_ε	$1.52 \cdot 10^{-3}$
λ_u	1.8cm
K	1.26
$\varepsilon_{x,y}$(normalized)	2mm·mrad

Table 4: LEUTL parameters.

E	217MeV
I	266A
σ_ε	10^{-3}
λ_u	3.3cm
K	3.1
$\varepsilon_{x,y}$(normalized)	5mm·mrad

the code, coincides with that calculated using a β just twice the average value occurring in the simulation.

To further support the validity of the present analysis, we have reported in Fig. 3 the saturation length vs β predicted for the case of VISA, whose parameters are given in Tab. 3. By evaluating L_s in the region of relevant β-values, we obtain a length of about 4m, which, compared with SPARC, is by no means surprising. One should, indeed, take into account that the length of the undulator period is significantly smaller than the SPARC value and the current is more than twice.

In Fig. 4 we have reported the same analysis for the LEUTL FEL. In this case too, we have found a satisfactory agreement with the experimental results (see Tab. 4 for the input parameters).

In the forthcoming sections we will use the above result as the starting point to fix the operating point of SPARC.

0.2 PRELIMINARY CONSIDERATIONS ON THE SPARC FEL WORKING POINTS

To give an idea of the sensitivity of the whole device to the main parameters of the system, we have reported in Fig. 5, the saturation length vs e-beam

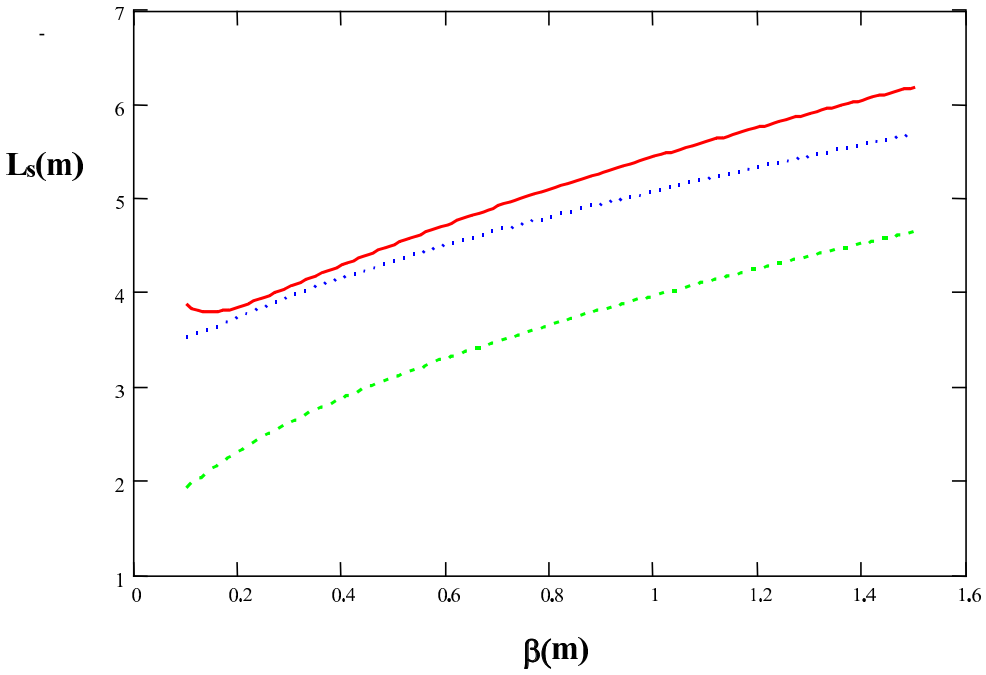

Figure 3: Same as Fig. 1 for the VISA case, input parameters from Tab. 3.

current, at different values of the emittance (1mm·mrad$\leq \varepsilon_n \leq$ 2mm·mrad) and energy spread ($0.6 \cdot 10^{-3} \leq \sigma_\varepsilon \leq 10^{-3}$), we should keep in mind that the values of L_s, reported in the figure, do not include the drift sections, which will be assumed to amount to a total length of about 2m, these values should be confronted with the presently available space $L^* = 14.5$m.

At 85A L_s is very close to L^*, even in the case of the design parameters reported in Tab. 1, no contingency is therefore left out, to be on the safe side in the hypothesis we get an e-beam with larger emittances and larger energy spread.

In the previous calculations we have assumed the undulator parameters given in Tab. 2 and we have considered a standard Halbach configuration, thus getting a first rough estimate of undulator performances and size from the formula [3]

$$B = 2B_r \frac{\sin\left(\frac{\pi}{M}\right)}{\frac{\pi}{M}} (1 - \exp(-2\pi \frac{h}{\lambda_u})) \exp(-\pi \frac{g}{\lambda_u}) \tag{6}$$

where B_r is the remanent field, M is the number of magnetic blocks per period, h the height of the single block and g the undulator gap.

In Fig. 6 we have reported the K parameter vs the gap by requiring a

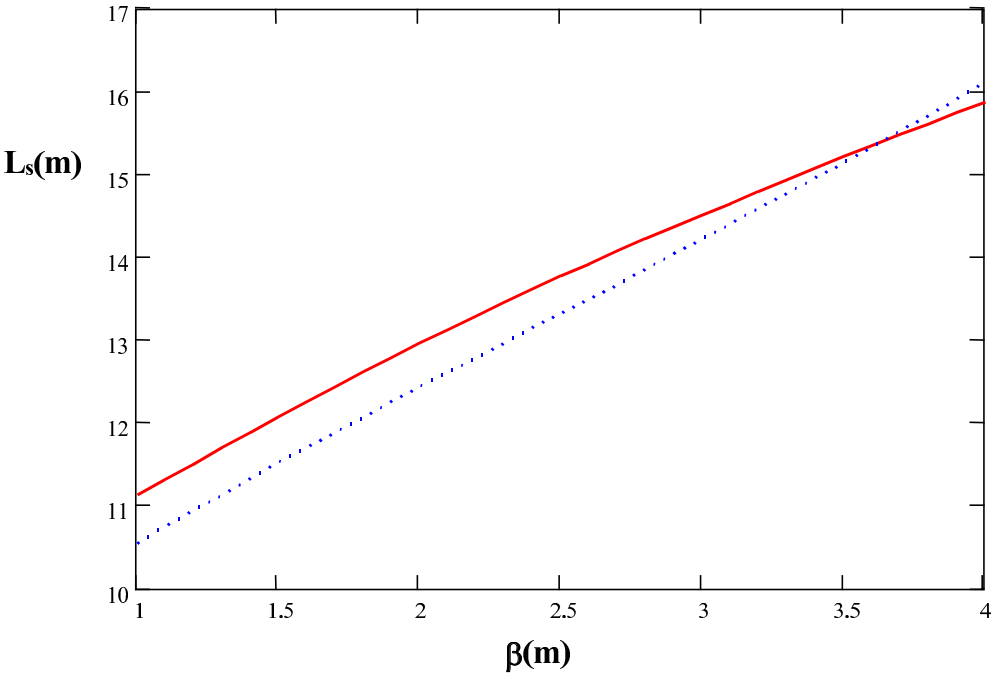

Figure 4: Same as Fig. 1 for the LEUTL case, input parameters from Tab. 4. The comparison with the case without diffraction has not been included.

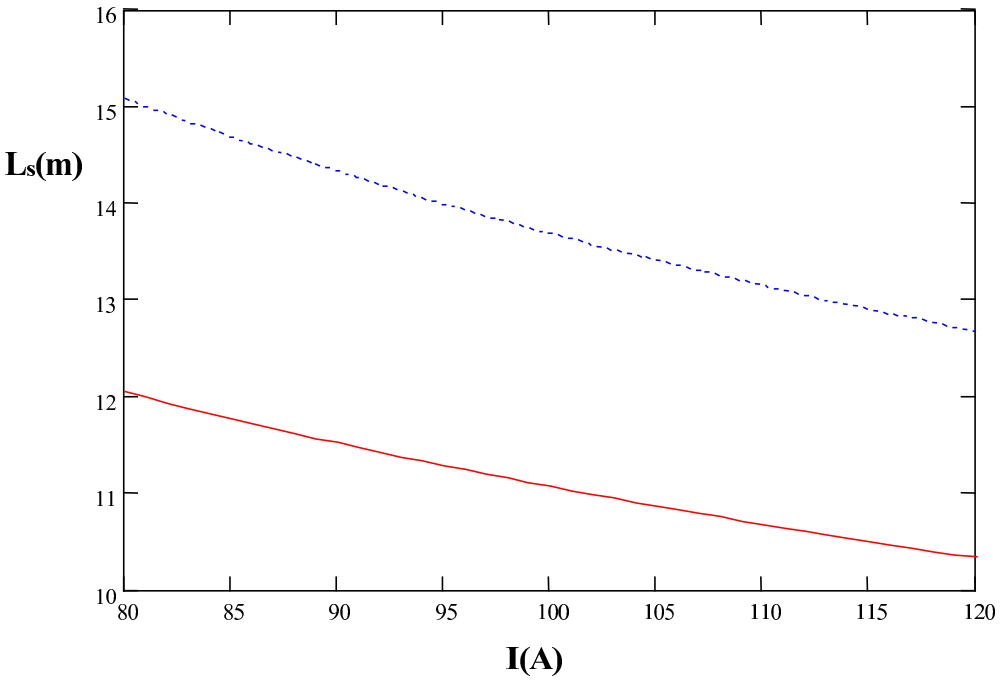

Figure 5: Saturation length vs current for $\lambda_u = 3$cm, $K = 2$, $E = 155.3$MeV. Dotted line $\sigma_\varepsilon = 10^{-3}$, $\varepsilon_{x,y} = 2$mm·mrad, solid line $\sigma_\varepsilon = 0.6 \cdot 10^{-3}$, $\varepsilon_{x,y} = 1$mm·mrad.

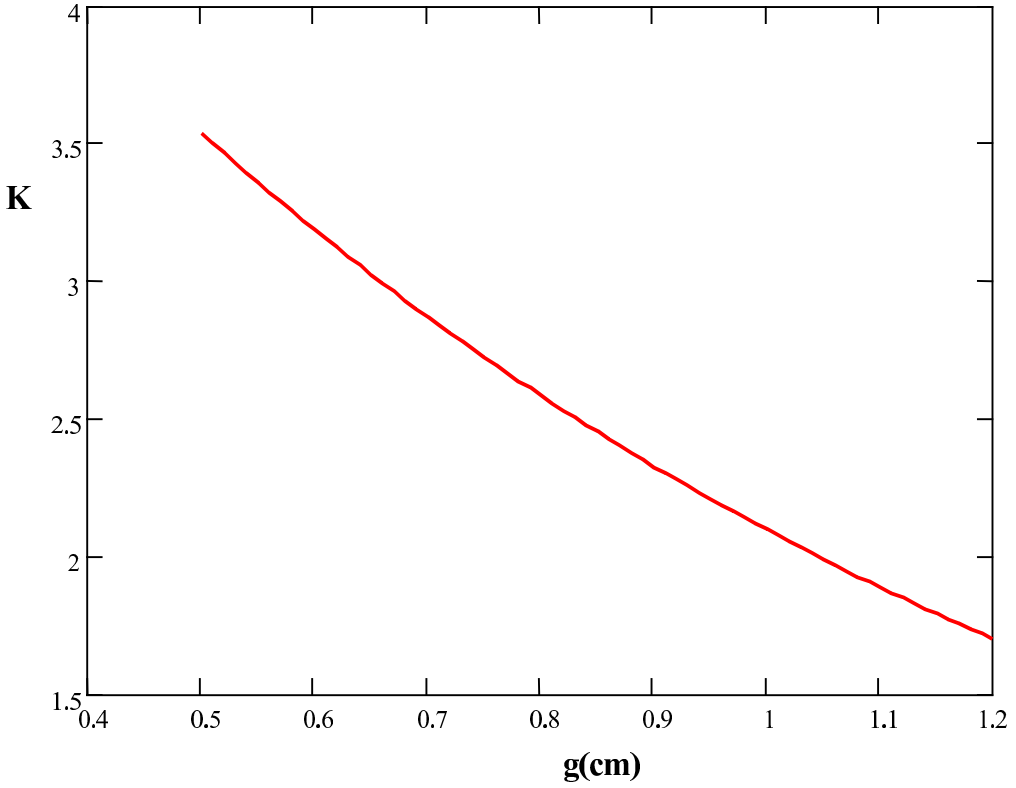

Figure 6: Undulator strength parameter K vs the gap for $B_r = 1.25$T, $\lambda_u = 3$cm, $h = \frac{\lambda_u}{2}$ and $M = 4$.

remanent field of 1.25T, $h = \frac{\lambda_u}{2}$, $M = 4$ we find $g \simeq 10$mm to obtain a value of K around 2.

A way to reduce the saturation length could be that of reducing the undulator period, this would demand for a smaller gap to ensure a reasonable value of the K parameter and thus sufficient gain at the SPARC e-beam energy values.

For e-beam transport reasons we can consider a safe region for FEL operation any undulator gap length not less than 9mm.

By keeping in mind such a constraint and that we are working with an e-beam enery of 155.3MeV, we can try a kind of optimization by exploiting eq. (6).

In Fig. 7 we have reported the analogous of Fig. 5, for the following undulator parameters: $\lambda_u = 2.8$cm, $K = 2.143$, ($g = 9$mm, $M = 4$, $h = 3.5$cm). It is evident that the operation at $I = 85$A is still problematic, even with a shorter undulator period.

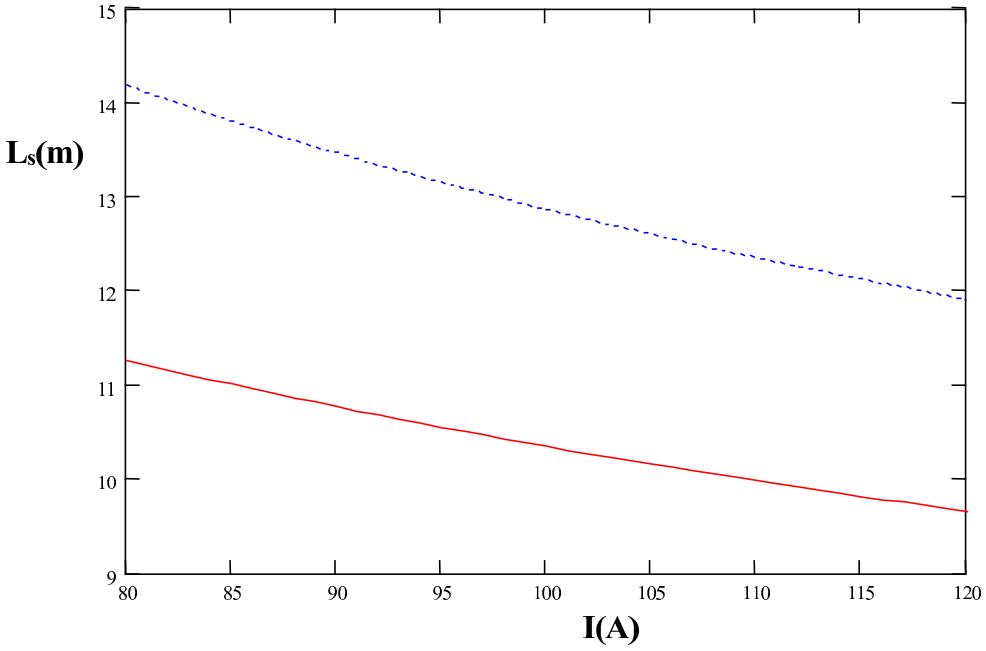

Figure 7: Same as Fig. 5 for $B_r = 1.25$T, $\lambda_u = 2.8$cm, $K = 2.143$

We can conclude, from this preliminary analysis, that an effort aimed at providing an e-beam peak current of 110A and a redesigning of the undulator could be the directions in which we can go to be on the safe side.

0.3 NUMERICAL ANALYSIS AND SPARC WORKING POINT

In this section we will reconsider the problem from a fully numerical point of view.

In Fig. 8 we have reported the growth of the FEL signal along the undulator, using the parameters of Tabs. 1,2.

It is to be noted that 5 drift sections, each one of 36cm, have been added to insert focusing elements; as schematically shown in figure.

We find that saturation occurs after more than 14m (including drift) and therefore full agreement with the results of the previous section is recovered.

In Fig. 9 we have reported the same of Fig. 8, for an e-beam with peak current equal to 110A, the results are again in agreement with the analytical estimates and we find, indeed, saturation in about 12m (including drifts).

In Figs. 10,11 we have reported the cases with $\lambda_u = 2.8$cm. In this case

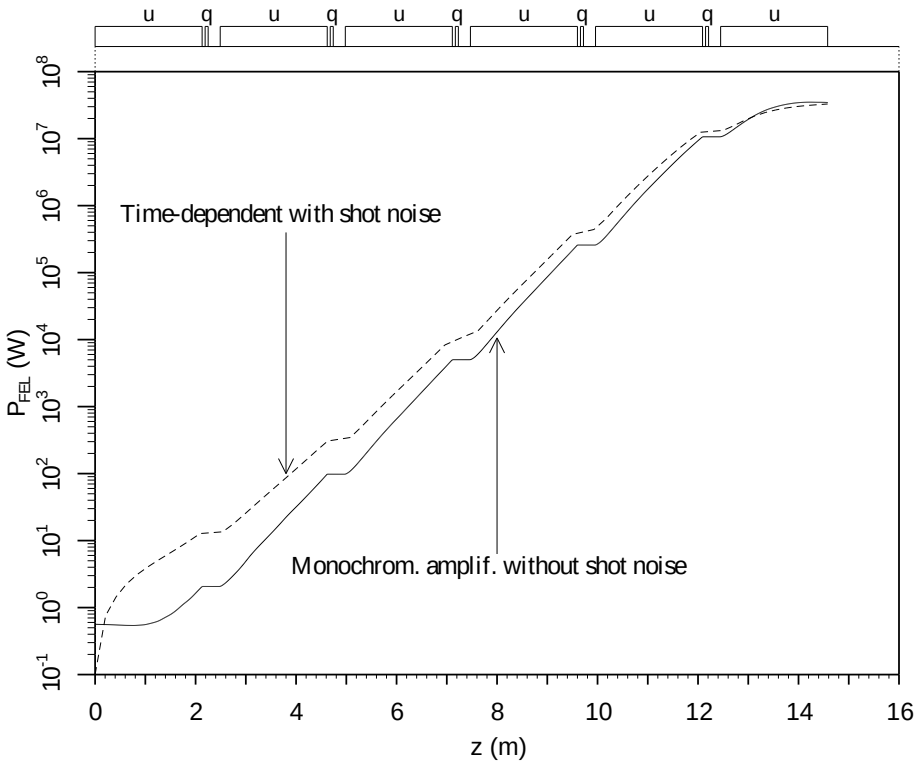

Figure 8: FEL power evolution vs the saturation distance. Ginger simulation input parameters from Tabs. 1,2 the undulator is not focusing in both directions and 5 drift section of 36cm have been included to insert quadrupoles.

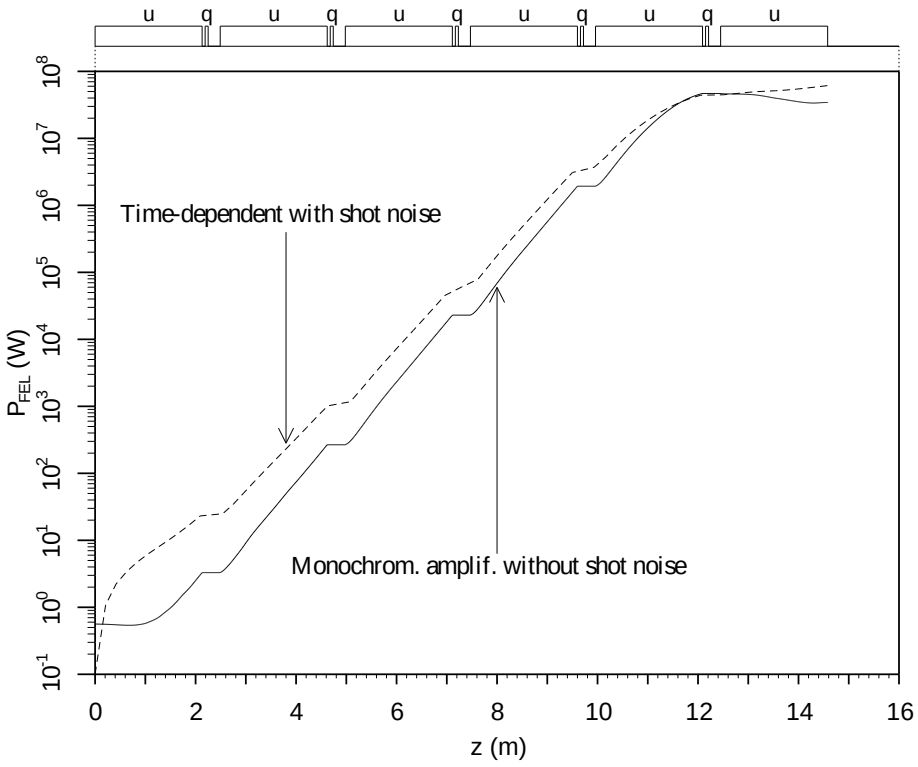

Figure 9: Same as Fig. 8 with $I = 110$A.

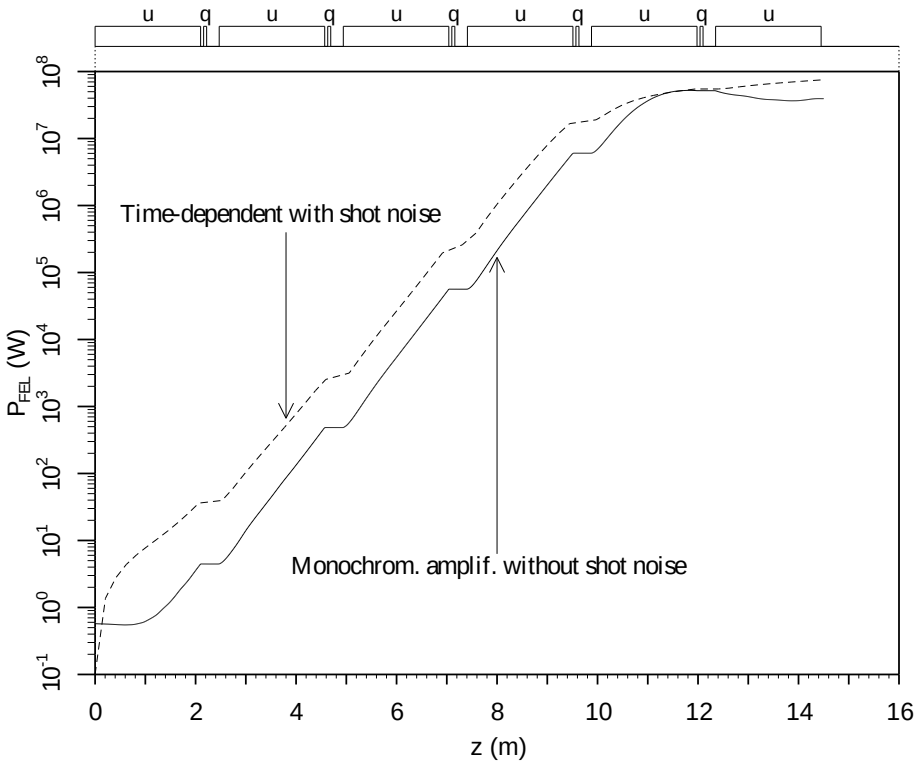

Figure 10: Same as Fig.8 for $\lambda_u = 2.8$cm, $K = 2.143$, $E = 155.3$MeV, $\sigma_\varepsilon = 0.6 \cdot 10^{-3}$, $\varepsilon_{x,y} = 1$mm·mrad and $I = 110$A.

too we may argue the same conclusions as before, namely the adjustment of the undulator parameters along with an increase of the e-beam current may leave a significant margin of contingency for the FEL operation.

In conclusion it would be desirable to work with the e-beam and undulator parameters of Fig. 10 and summarized in Tab. 5, to operate on the safe side.

0.4 CONCLUDING REMARKS

It is important to stress that three constraints have guided the present analysis:

1. saturation length not longer than 14.5m;

2. undulator gap not less than 9mm;

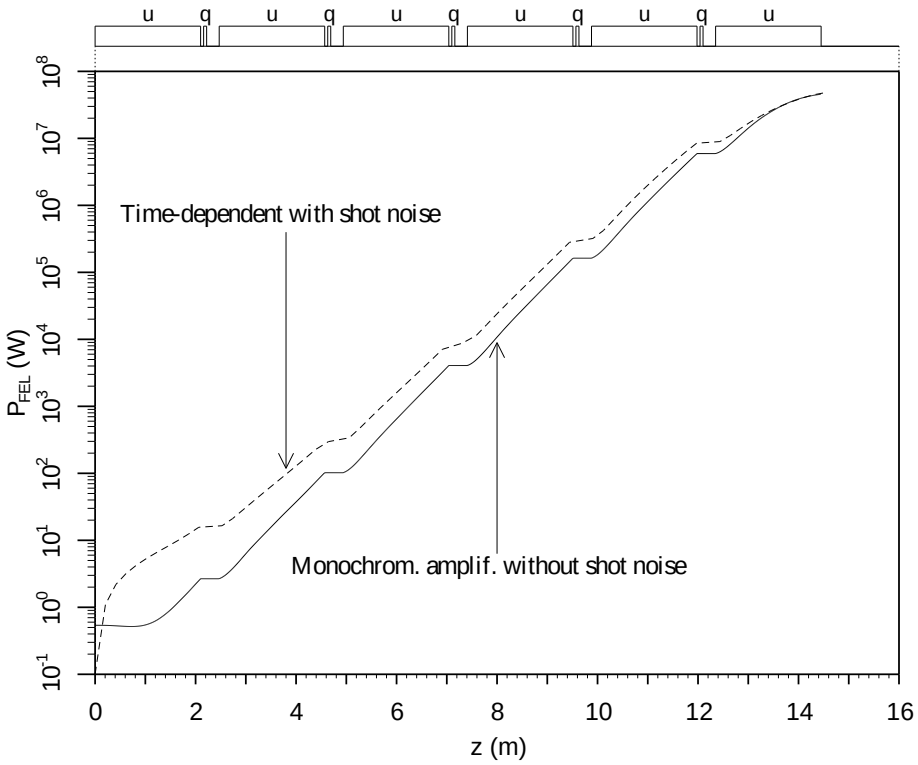

Figure 11: Same as Fig. 10 for $\sigma_\varepsilon = 10^{-3}$, $\varepsilon_{x,y} = 2$mm·mrad.

Table 5: SPARC parameters, tentative configuration.

E	155.3MeV
I	110A
σ_ε	$0.6 \cdot 10^{-3}$
$\varepsilon_{x,y}$(normalized)	1mm·mrad
λ_u	2.8cm
K	2.143

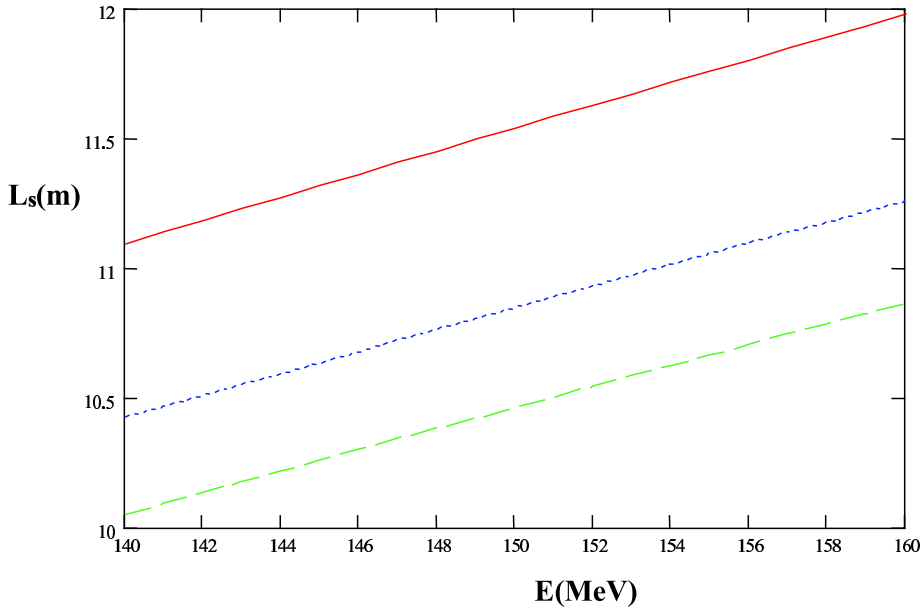

Figure 12: Saturation length vs energy for different values of the current. Solid 85A, dotted 100A, dashed 110A and parameters of Tab. 5.

3. electron beam energy around 155MeV.

If we relax the third conditions, which implies FEL operation slightly above 500nm, we can add a further element to the discussion concerning the possibility of working at lower energies.

In Fig. 12 we have reported the analogous of Fig. 5, regarding the dependence of the saturation length vs energy for different current values. It is evident that working e. g. with $I = 100$A and using the parameters of Tab. 5 for the undulator we find saturation length (without the inclusion of drift sections) not exceeding 11m (for energy below 155MeV).

This configuration of parameters seem to be safe from the point of view of the contingency and sufficient margin is left out in the hypothesis that one gets a larger emittance (within a factor of two larger than the design value) or a larger energy spread (up to 10^{-3}).

Other solutions can be considered to reduce the saturation length and one of these is briefly described below.

We have indeed considered the possibility of exploiting different undulator schemes. In particular we have studied the case of a "hybrid" segmented solution consisting of a combination of a helical and a linear sections [4].

The first part, namely the helical section, is used as modulator, to bunch the electrons, the second part linear, is used as radiator and here higher order non-linear harmonics can be generated. The length of the radiator is much shorter than the modulator. For this reason such a configuration can be exploited to reduce the saturation length of the device. The gain of the system associated in the helical section is, indeed larger than the linear part (for the details see ref. [4]).

Even though interesting, this solution for SPARC is not possible, being the necessary on axis magnetic fields of the modulator section achieved for small gap values (below 8mm).

In conclusions, we can state that if SPARC will be operated with the parameters of Tabs. 1,2, the present space of 14.5m to allocate undulator and drift sections does not provide sufficient margin to reach full saturation and test the non-linear harmonic generation. Furthermore no contingency is left out in the case in which larger emittances and larger energy spread are obtained. It will be therefore necessary to gain extra-space to include an other undulator section.

It should also be noted that, in the present design of the 6m transport channel from the linac to the undulator, the space (3.8m), needed to place the deflecting magnet, is large and it is therefore necessary to allocate the triplets of quadrupoles at the output of the linac and at the input of the undulator, very close (0.2m) to the linac and to the undulator respectively. This fact may create problems to the insertion of correcting coils and diagnostic elements.

A reconsideration of these spaces could be helpful to overcome this problem and to save extra-space for further undulator elements.

This aspect of the problem deserves a more careful analysis which will be discussed in a separated report.

Bibliography

[1] G. Dattoli, L. Giannessi, P. L. Ottaviani and C. Ronsivalle:
J. Appl. Phys. to be published.

[2] SPARC-PHASE-1 Parameter Table, Distributed by L. Serafini
(release 1 March 20 2003).

[3] F. Ciocci, G. Dattoli, A. Torre and A. Renieri:
"Insertion Devices and Free Electron Lasers"
World Scientific, Singapore 2000.

[4] S. G. Biedron, G. Dattoli, H. P. Freund, L. Mezi and P. L. Ottaviani:
Phys. Rev. E to be publihed.